REFERENCE 138

J. R. DOMINEY, R. C. LANE, AND A. F. THOMAS, "CRITICAL MASS MEASUREMENTS WITH THIN DISCS OF 45.5% ENRICHED URANIUM, " UNITED KINGDOM ATOMIC ENERGY AUTHORITY REPORT AWRE NR/A-1/62, ALDERMASTON (JANUARY 1962).

AWRE NR/A - 1/62

AWRE NR/A - 1/62

35 Pages

UNITED KINGDOM ATOMIC ENERGY AUTHORITY

ATOMIC WEAPONS RESEARCH ESTABLISHMENT

AWRE REPORT No. NR/A - 1/62

Critical Mass Measurements with Thin Discs of 45.5% Enriched Uranium

J. R. Dominey
R. C. Lane
A. F. Thomas

A.W.R.E.,
Aldermaston, Berks.

March 1962

United Kingdom Atomic Energy Authority

ATOMIC WEAPONS RESEARCH ESTABLISHMENT

AWRE REPORT NO. NR/A-1/62

Critical Mass Measurements with Thin Discs of 45.5% Enriched Uranium

J. R. Dominey
R. C. Lane
A. F. Thomas

Summary

Critical masses of cylinders of 45.5% enriched uranium have been measured for systems with effective radii of 5.79, 8.46 and 11.05 in. Measurements were made for "bare" systems and for systems reflected by natural uranium, graphite, borated graphite, steel and aluminium. The results obtained gave critical masses in the height/diameter ratio range of 0.08 to 0.63, and these results are correlated by the use of an equal geometric buckling conversion.

Recommended for issue by

J. J. McEnhill, Superintendent

Approved by

K. W. Allen, Senior Superintendent

539.175.2.09.083:N.543.462
N.543.462:539.175.2.09.083

TABLE OF CONTENTS

1. INTRODUCTION

Experimental values of critical masses of near isometric cylinders or spheres of uranium of various enrichments have been published [1 - 3]. In the safety evaluation of certain manufacturing processes a knowledge of the critical masses of non-isometric cylinders or slabs is required. Accordingly, using a supply of 45% enriched uranium, which became available for a short period, a series of measurements was made at AWRE, Aldermaston on the critical heights of cylinders of H/D ratios between 0.08 and 0.63.

This report describes these measurements and constants are deduced correlating the experimental data, by means of the equal Geometrical Buckling conversion, which, at least, enable values of critical masses of cylinders within the experimental range of H/D values to be computed quickly and tolerably accurately.

2. CRITICAL ASSEMBLY MACHINE AND INSTRUMENTATION

2.1 Assembly Machine - Atlas

The "approach-to-critical" machine, Atlas, was used for these experiments. Atlas is shown in Figure 1. It has a total load carrying capacity of 5 tons, the load being equally distributed between the two platforms. Assemblies up to approximately 5 ft in diameter may be built on either platform. The fixed upper platform is mounted securely on two 10 ft high main stanchions. Accurately machined guide rails are secured on these stanchions. The lower platform travels vertically between the main stanchions, and is located laterally by roller bearings travelling on the machined guide rails. The lower platform is mounted on a 4 in. diameter hydraulic ram, which is supplied with oil at a pressure up to 2000 p.s.i. The lower platform has a maximum travel of 68 in., and has a maximum rate of rise of ½ in./s. The position of the lower platform is indicated in 0.1 in. steps by a Veeder-Roote counter, driven by a rotating contact on the platform.

Precise control of the upward movement of the lower platform is provided by phosphor bronze pads located on three vertical lead-screws. The three lead-screws are geared together and driven by a Varimag electric motor unit. Interlocks are provided to ensure that the platform remains in contact with the pads during upward movement. The rate of rise of the lower platform when in contact with the pads

is continuously variable from 0.075 to 4.5 in./min. The position of the pads, and hence of the platform when in contact, is displayed by a Magslip transmitter-receiver sytem, which can be read to 0.002 in.

To ensure that any assembly can be rapidly dismantled, a magnetically held valve is incorporated in the hydraulic circuit. Interruption of the electrical supply to this valve thus allows the lower platform to fall freely. The platform starts to fall about 100 ms after the supply is interrupted, and rapidly accelerates to a maximum speed of about 7 in./s. Over the last 15 in. of fall, the platform is progressively retarded to prevent shock to the components.

2.2 Instrumentation

All assemblies were monitored by 3 neutron counting channels, of which two had to be fully operational at any stage during an approach-to-critical run. The neutron detectors were enriched BF_3 proportional counters used in standard AWRE "long counter geometry" [4]. If the recorded count rate in any channel exceeded a pre-determined level, an electronic "trip unit" would operate, releasing the lower platform of Atlas as described in Section 2.1.

3. ASSEMBLY COMPONENTS

3.1 Enriched Uranium

Approximately 470 kg of 45.5 ± 0.46% enriched uranium were available for these experiments. This material was cast and, where necessary, machined into hexagons or half-hexagons. The details of the hexagons produced are given in Table 1.

All enriched uranium components were lacquered with approximately 0.001 in. of yellow lacquer. This lacquer served two purposes:-

(a) It prevented any spread of contamination.

(b) It prevented any confusion between enriched and natural uranium components.

In this series of experiments, the hexagons and half-hexagons were assembled into pseudo-cylinders as shown in Figure 2. The effective radii quoted are the radii of cylinders with the same cross-sectional area.

The overall packing density of the enriched uranium in these pseudo-cylinders was 98 - 99%. This gave an effective density for the enriched uranium assemblies of 18.16 ± 0.09 g/cm^3.

3.2 Natural Uranium Reflector

The side reflectors were assembled from hexagons and half-hexagons of natural uranium, which were manufactured to the same dimensions as the enriched uranium components described in Section 3.1. These were placed round the sides of the enriched uranium pseudo-cylinders as shown in Figure 3, giving a radial reflector 7.05 in. wide and with an effective density of 18.26 ± 0.13 g/cm^3.

The top and bottom reflectors of natural uranium were assembled in steel boxes. The reflectors were constructed from rods and slabs of natural uranium, the rods being 6 in. long and 1.2 in. diameter while the slabs were 12 in. long by 6 in. wide by 1 in. thick.

The overall composition of the top and bottom natural uranium reflectors was as given in Tables 2 and 3.

Figure 4 shows the bottom and side reflectors of natural uranium, and Figure 5 shows the structure of the upper uranium reflector.

3.3 Graphite Reflector

Side reflectors of graphite were cut in two patterns, as shown in Figure 6. As shown in this figure, combinations of these components could be used to reflect the side faces of the pseudo-cylinders by approximately 6 in. of graphite. The packing density of these side reflectors was effectively 100%, and the mean side reflector density was therefore 1.74 ± 0.03 g/cm^3

The top and bottom face graphite reflectors were constructed from graphite blocks, 12 in. long by 6 in. square. These blocks were placed in the steel boxes described in Section 3.2. Thus the mean compositions of the top and bottom graphite reflectors were as given in Tables 4 and 5.

3.4 "Borated Graphite" Reflector

The side reflectors for this assembly were constructed of graphite, as described in Section 3.4.

The top "borated graphite" reflector was constructed from 8 in. square blocks of borated graphite, density 1.74 ± 0.06 g/cm^3. The composition of this borated graphite is given in Table 6.

The blocks were assembled on a 0.375 in. thick aluminium alloy plate; the blocks covered an area greater than 40 in. square. The mean packing density was 89%, giving an effective borated graphite reflector density of 1.55 ± 0.05 g/cm^3.

The bottom "borated graphite" reflector was again constructed from 8 in. square blocks, assembled together to give an assembly greater than 40 in. square, with an effective density of 1.55 ± 0.05 g/cm^3. A steel plate, 0.067 in. thick, placed on top of these blocks gave a smooth surface for assembly of the fissile material.

3.5 Aluminium Reflector

The aluminium side reflectors were constructed from pieces of aluminium cut to the same dimensions as the graphite components described in Section 3.3. The effective density of the side reflector was thus 2.72 ± 0.03 g/cm^3. An illustration of an aluminium reflected pseudo-cylinder, showing the side reflectors, is given in Figures 7 and 8.

The upper aluminium reflector consisted of twelve 6 in. square aluminium blocks, each 18 in. long, supported on a larger aluminium plate 0.377 in. thick.

The lower aluminium reflector consisted of six 1 in. thick aluminium plates, each 36 in. square, securely bolted together.

The effective density of the upper and lower aluminium reflectors was 2.58 ± 0.03 g/cm^3.

The complete aluminium reflected assembly is shown in Figure 9.

3.6 Steel Reflector

The steel side reflectors were constructed from pieces of mild steel cut to the same dimensions as those graphite components described in Section 3.3. The effective density of the side reflector was 7.78 ± 0.02 g/cm^3.

The upper steel reflector consisted of eighteen

6 in. square steel blocks, each 12 in. long, supported on a large steel plate 0.558 in. thick.

The lower steel reflector consisted of six 1 in. thick steel plates, each 36 in. square, securely bolted together.

The mean density of the upper and lower steel reflectors was 7.24 ± 0.02 g/cm^3.

3.7 Jig for Studying "Bare", i.e., Unreflected, Systems

To study "bare" systems, the fissile material was divided into two approximately equal components.

Both upper and lower components were supported on aluminium plates 0.186 in. thick. The plates in turn were supported by a framework of aluminium angle. This reduced neutron reflection to the practical minimum.

Two views of "bare" assemblies are shown in Figures 10 and 11.

4. EXPERIMENTAL PROCEDURE

4.1 "Normalising" and "Live" Runs

The procedure adopted for demonstrating whether a given system is sub-critical or not is as follows. The system is split into sub-assemblies, each of which is demonstrably sub-critical and safe to handle, both in isolation and at reasonable separations (~ 5 ft) from an identical component. A replica of these sub-assemblies is then built from non-fissile material (usually natural uranium or graphite) on both the upper and lower platforms of Atlas. A mock fission neutron source is situated near or inside one assembly. A "normalising curve" is then derived by measuring the neutron output of the system as the two components are brought together. This "normalising curve", giving the variation of response of the various counters with separation of components, allows for any changes in neutron output with a fissile system due to geometry changes alone.

The lower platform is then dropped to its lowest position, and the replicas replaced by fissile material. The neutron output of this "live" system is then monitored as the two components are brought gradually together. At a given separation of the components, the ratio, R, between the "live" and "normalising" counts gives a measure of the

neutron multiplication of the system. When a system is just delayed critical, the neutron multiplication becomes infinite, and hence R^{-1} becomes zero. Thus, by plotting R^{-1} against separation, the safety of successive steps may be assessed; eventually, if the system is closed with a finite value of R, the system is sub-critical. If, however, the R^{-1} plot indicates that R^{-1} would be zero at a finite separation, the system would be super-critical when fully assembled.

Thus a series of "normalising" and "live" runs may be used to demonstrate the state of criticality of any given system.

4.2 Estimation of Critical Dimensions

If, as in this experiment, one dimension, i.e., the height of a given pseudo-cylinder, is variable in small steps, the procedure usually adopted is to establish two values of this parameter, namely:-

(a) The minimum height which, if fully assembled, would be just super-critical.

(b) The maximum height which, when fully assembled, is sub-critical.

These two values differing by the smallest height increment available, specify the critical height to within the limit of this increment. To predict the critical height more accurately, the following procedure is adopted.

The neutron multiplications of a series of systems are measured, starting with that system ((b) above) which is just sub-critical when fully assembled, and reducing the height in successive small steps. Then by plotting the reciprocal neutron multiplication against height and extrapolating to zero reciprocal neutron multiplication, one may predict the critical height.

4.3 Corrections for Container Interfaces

In three assemblies, namely "bare", natural uranium and graphite reflected, a steel or aluminium interface was between the fissile component and the upper or lower assembly. Subsidiary experiments were carried out to measure the effects of these interfaces.

5. EXPERIMENTAL RESULTS

Tables 7 to 12 give the neutron multiplication

measurements made with each system. The errors quoted on the reciprocal multiplication are only those arising from the counting statistics - no attempt was made to assess experimental errors by checking reproducibility, etc. The subsidiary experiments with natural uranium and graphite reflectors to determine the effect of the steel interfaces showed that this introduced an error of less than ½% in the extrapolated critical heights.

Figures 11 and 12 give graphs of reciprocal neutron multiplication against slab height for each reflector system. Also shown are the extrapolations to give the critical heights.

Table 13 gives the estimated critical height for each of the systems studied. The errors quoted on the critical heights define the upper and lower limits of extrapolation considered to be consistent with the experimental results.

6. DISCUSSION OF THE EXPERIMENTAL RESULTS

The results obtained in these experiments provide data on critical systems at more extreme height-diameter ratios than have previously been studied at medium enrichment. Their usefulness may be extended by interpolation, and, with less confidence, by extrapolation. The choice of method of interpolation is arbitrary - Equal Geometrical Buckling conversion, plotting critical height again n/1 + n (where n = height/diameter) and plotting critical height against critical area are possible methods, but the first offers some advantages in combining the results with different reflectors and of simplicity in extrapolation.

The one-group form of the equal buckling relation is

$$B^2 = \frac{\pi^2}{(R + \lambda_0)^2} = \frac{\pi^2}{(H + 2\lambda_1)^2} + \frac{4.81^2}{(D + 2\lambda_2)^2} = \frac{\pi^2}{(T + 2\lambda_3)^2},$$

where R is the radius of the critical sphere;

H is the critical height of the cylinder, diameter D;

T is the thickness of the critical infinite slab;

and λ_0, λ_1, λ_2, λ_3, are appropriate constants.

Values of B^2 and λ which gave the best least squares fit to the results were calculated; except for the uranium

reflected system and the borated graphite reflected system (in which the radial and axial reflectors differed) λ_1 and λ_2 were taken to be equal. The values were calculated in two sets:-

(a) Values of B^2 and λ to give the best fit to the results obtained for each reflector separately.

(b) Values of λ appropriate to each reflector, which when combined with a unique value of B^2, gave the best fit.

The values of B^2 and λ are given in Table 14, together with the critical heights predicted by these values at the experimental diameters. As will be seen, there is little to choose between the two methods - the latter affords some simplicity.

Values of the thickness of the critical infinite slab and of the radius and mass of the critical sphere, calculated from the values of B^2 and λ of Set (b) and assuming $\lambda_0 = \lambda_1 = \lambda_2 = \lambda_3$, are given in Table 15.

Experimental data are not available to check the adequacy of these extrapolations directly. However, Paxton [2] quotes empirical relations which, when combined with data on near isometric critical systems at 37½% and 54% enrichment, give estimates of the critical parameter for a sphere at 45% enrichment for unreflected and natural uranium reflected systems. The critical masses deduced in this manner are 190 kg and 78 kg respectively.

As the validity of applying the correlation to extreme shapes, e.g., infinite slabs, has not been tested, its use for this purpose cannot be recommended, and the values given in Table 15 should be treated as affording only a comparison between the reflectors.

7. ACKNOWLEDGMENTS

The authors wish to acknowledge the assistance of Mr. H. Goodfellow in the conception and design of these experiments, and the assistance of Mr. O. J. E. Perkins, who directed the experimental team.

REFERENCES

1. Reactor Physics Constants. ANL5800.

2. Critical Masses of Fissionable Metals as Basic Nuclear Safety Data. LA1958.

3. Nuclear Safety Guide. TID7016.

4. "A Study of the Neutron Long Counter". AWRE Report No. NR/A-1/59.

TABLE 1

Whole Hexagons across Flat Dimension, in.	Half-Hexagons Flat to Diameter Dimension, in.	Thickness, in.	Mass, g	No. Produced
2.752 ± 0.005	-	1.215 ± 0.005	2413.8 ± 15.0	84
* -	1.351 ± 0.017	1.215 ± 0.005	1173.5 ± 18.9	60
2.761 ± 0.004	-	0.613 ± 0.004	1215.3 ± 10.2	110
* -	1.362 ± 0.002	0.613 ± 0.004	591.6 ± 5.6	24
2.757 ± 0.004	-	0.207 ± 0.002	411.4 ± 3.7	110
* -	1.344 ± 0.007	0.207 ± 0.001	201.9 ± 1.9	12

*The half-hexagons were produced by cutting across full hexagons by a thin milling tool. Hence the flat to diameter dimension is less than half the across flat dimension.

TABLE 2

Lower Natural Uranium Reflector

Layer No.*	Thickness, in.	Composition	Mean Density, g/cm^3
1	0.067	Mild Steel	7.78 ± 0.02
2	1.00	Natural Uranium	18.54 ± 0.06
3	5.67	Natural Uranium	16.07 ± 0.13

*Layers with lowest number nearest to fissile components.

TABLE 3

Upper Natural Uranium Reflector

Layer-No.*	Thick-ness, in.	Composition	Mean Density, g/cm^3
1	0.130	Mild Steel	7.78 ± 0.02
2	1.00	(i) Natural Uranium 98.0% by volume (ii) Mild Steel 2.0% by volume	18.33 ± 0.10
3	5.67	(iii) Natural Uranium 83.7% by volume (iv) Mild Steel 2.0% by volume	15.91 ± 0.16

*Layers with lowest numbers were nearest to fissile components.

TABLE 4

Upper Graphite Reflector

Layer No.	Thickness, in.	Composition	Mean Density, g/cm^3
1*	0.130	Mild Steel	7.78 ± 0.02
2	6.00	(i) Graphite 98.0% by volume (ii) Mild Steel 2.0% by volume	1.86 ± 0.04
*Layer No. 1 was next to the fissile components.			

TABLE 5

Lower Graphite Reflector

Layer No.	Thickness, in.	Composition	Mean Density, g/cm^3
1*	0.067	Mild Steel	7.78
2	6.00	Graphite	1.74 ± 0.03
*Layer No. 1 was next to the fissile components.			

TABLE 6

Composition of Borated Graphite

Boron, expressed as $Na_2B_4O_7$	26.50 ± 0.8%
Carbon	71.45 ± 2.5%
Water	3.85 ± 0.1%

TABLE 7

Neutron Multiplication Measurements with "Bare" Slabs of 45.5% Enriched Uranium

Slab Thickness, in.	Interfaces, in. of Aluminium	Inverse Neutron Multiplication					
		Effective Radius of Slab, in.					
		5.79			8.46		
		Counter 1	Counter 2	Counter 3	Counter 1	Counter 2	Counter 3
6.075 ± 0.011	3/8	0.0990 ± 0.0014	0.1032 ± 0.0014	0.1271 ± 0.0006	-	-	-
	3/16	0.0884 ± 0.0013	0.0890 ± 0.0013	0.1156 ± 0.0006			
	* Zero	0.0778 ± 0.0019	0.0748 ± 0.0019	0.1041 ± 0.0008			
6.688 ± 0.012	3/8	0.0559 ± 0.0008	0.0568 ± 0.0008	0.0781 ± 0.0004	-	-	-
	3/16	0.0449 ± 0.0006	0.0446 ± 0.0006	0.0616 ± 0.0003			
	* Zero	0.0339 ± 0.0010	0.0324 ± 0.0010	0.0451 ± 0.0005			
6.895 ± 0.012	3/8	0.0441 ± 0.0006	0.0441 ± 0.0006	0.0580 ± 0.0003	-	-	-
	3/16	0.0326 ± 0.0005	0.0326 ± 0.0004	0.0435 ± 0.0002			
	* Zero	0.0211 ± 0.0008	0.0211 ± 0.0007	0.0290 ± 0.0004			
7.102 ± 0.012	3/8	0.0340 ± 0.0005	0.0340 ± 0.0005	0.0431 ± 0.0002	-	-	-
	3/16	0.0210 ± 0.0003	0.0209 ± 0.0003	0.0279 ± 0.0001			
	* Zero	0.0080 ± 0.0006	0.0078 ± 0.0006	0.0127 ± 0.0002			
7.311 ± 0.012	3/8	0.0248 ± 0.0003	0.0244 ± 0.0003	0.0296 ± 0.0002	-	-	-
	3/16	0.0104 ± 0.0001	0.0104 ± 0.0001	0.0132 ± 0.0001			
	* Zero	-0.0040 ± 0.0003	-0.0036 ± 0.0003	-0.0032 ± 0.0002			
4.258 ± 0.010	3/8	-	-	-	0.1557 ± 0.0035	0.1498 ± 0.0028	0.2151 ± 0.0011
	3/16				0.1461 ± 0.0030	0.1462 ± 0.0028	0.2026 ± 0.0010
	* Zero				0.1365 ± 0.0055	0.1426 ± 0.0049	0.1901 ± 0.0018
4.882 ± 0.011	3/8	-	-	-	0.0784 ± 0.0015	0.0765 ± 0.0014	0.1165 ± 0.0006
	3/16				0.0659 ± 0.0013	0.0687 ± 0.0012	0.1059 ± 0.0005
	* Zero				0.0534 ± 0.0024	0.0609 ± 0.0022	0.0953 ± 0.0009
5.089 ± 0.011	3/8	-	-	-	0.0554 ± 0.0011	0.0545 ± 0.0010	0.0844 ± 0.0004
	3/16				0.0433 ± 0.0007	0.0458 ± 0.0007	0.0724 ± 0.0002
	* Zero				0.0312 ± 0.0015	0.0375 ± 0.0014	0.0604 ± 0.0005
5.296 ± 0.011	3/8	-	-	-	0.0331 ± 0.0007	0.0336 ± 0.0006	0.0541 ± 0.0003
	3/16				0.0232 ± 0.0005	0.0262 ± 0.0005	0.0412 ± 0.0002
	* Zero				0.0133 ± 0.0010	0.0188 ± 0.0009	0.0283 ± 0.0005

* Extrapolated from results with 3/8 and 3/16 in. of aluminium.

TABLE 8

Neutron Multiplication Measurements with 45.5% Enriched U-235 Slabs Reflected on all Faces by Graphite

Slab Thickness, in.	Inverse Neutron Multiplication								
	Effective Radius of Slab, in.								
	5.79			8.46			11.05		
	Counter 1	Counter 2	Counter 3	Counter 1	Counter 2	Counter 3	Counter 1	Counter 2	Counter 3
1.215 ± 0.005	0.4067 ± 0.0071	0.3973 ± 0.0065	0.4590 ± 0.0010	0.2602 ± 0.0048	0.2710 ± 0.0048	0.3244 ± 0.0008	0.1628 ± 0.0027	0.1794 ± 0.0028	0.2366 ± 0.0014
1.422 ± 0.005	-	-	-	0.1817 ± 0.0033	0.1876 ± 0.0033	0.2328 ± 0.0005	0.0884 ± 0.0016	0.1009 ± 0.0016	0.1332 ± 0.0003
1.629 ± 0.006	-	-	-	0.1213 ± 0.0021	0.1309 ± 0.0022	0.1563 ± 0.0009	0.0349 ± 0.0006	0.0382 ± 0.0006	0.0557 ± 0.0001
1.828 ± 0.006	0.2181 ± 0.0034	0.2247 ± 0.0025	0.2749 ± 0.0006	0.0690 ± 0.0011	0.0726 ± 0.0013	0.0994 ± 0.0002	-	-	-
2.035 ± 0.007	-	-	-	0.0223 ± 0.0004	0.0239 ± 0.0004	0.0321 ± 0.0001	-	-	-
2.428 ± 0.007	0.0873 ± 0.0012	0.0965 ± 0.0014	0.1186 ± 0.0002	-	-	-	-	-	-
2.842 ± 0.008	0.0227 ± 0.0002	0.0249 ± 0.0003	0.0311 ± 0.0001	-	-	-	-	-	-

TABLE 9

Neutron Multiplication Measurements with 45.5% Enriched U-235 Slabs Reflected on Slab Faces by Borated Graphite and on Side Faces by Graphite

Slab Thickness, in.	Inverse Neutron Multiplication								
	Effective Radius of Slab, in.								
	5.79			8.46			11.05		
	Counter 1	Counter 2	Counter 3	Counter 1	Counter 2	Counter 3	Counter 1	Counter 2	Counter 3
1.215 ± 0.005	-	-	-	0.3303 ± 0.0139	0.3826 ± 0.0140	0.4270 ± 0.0026	0.2701 ± 0.0116	0.2958 ± 0.0108	0.3605 ± 0.0021
1.422 ± 0.005	-	-	-	-	-	-	0.2044 ± 0.0083	0.2279 ± 0.0080	0.2994 ± 0.0017
1.629 ± 0.006	-	-	-	-	-	-	0.1467 ± 0.0057	0.1578 ± 0.0059	0.2178 ± 0.0012
1.828 ± 0.006	0.3283 ± 0.0135	0.3070 ± 0.0110	0.3471 ± 0.0036	0.1738 ± 0.0066	0.1839 ± 0.0066	0.2371 ± 0.0013	0.0998 ± 0.0037	0.1117 ± 0.0038	0.1581 ± 0.0008
2.035 ± 0.007	-	-	-	-	-	-	0.0538 ± 0.0021	0.0640 ± 0.0023	0.0950 ± 0.0005
2.242 ± 0.007	-	-	-	-	-	-	0.0219 ± 0.0008	0.0270 ± 0.0010	0.0425 ± 0.0002
2.430 ± 0.007	0.1767 ± 0.0062	0.1837 ± 0.0074	0.2148 ± 0.0013	0.0492 ± 0.0018	0.0536 ± 0.0019	0.0745 ± 0.0004	-	-	-
2.637 ± 0.007	-	-	-	0.0190 ± 0.0007	0.0232 ± 0.0008	0.0327 ± 0.0002	-	-	-
3.043 ± 0.008	0.0826 ± 0.0026	0.0819 ± 0.0033	0.1059 ± 0.0008	-	-	-	-	-	-
3.645 ± 0.009	0.0130 ± 0.0003	0.0132 ± 0.0004	0.0179 ± 0.0002	-	-	-	-	-	-

TABLE 10

Neutron Multiplication Measurements with 45.5% Enriched U-235 Slabs, Reflected on all Faces by Natural Uranium

Slab Thickness, in.	Inverse Neutron Multiplication								
	Effective Radius of Slab, in.								
	5.79			8.46			11.05		
	Counter 1	Counter 2	Counter 3	Counter 1	Counter 2	Counter 3	Counter 1	Counter 2	Counter 3
1.215 ± 0.005	0.4431 ± 0.0159	0.4472 ± 0.0145	0.5102 ± 0.0015	0.3605 ± 0.0116	0.3615 ± 0.0097	0.4072 ± 0.0012	0.2152 ± 0.0087	0.2284 ± 0.0081	0.3504 ± 0.0009
1.422 ± 0.005	-	-	-	-	-	-	0.1538 ± 0.0058	0.1818 ± 0.0050	0.2582 ± 0.0007
1.629 ± 0.006	-	-	-	-	-	-	0.1014 ± 0.0036	0.1174 ± 0.0031	0.1697 ± 0.0005
1.828 ± 0.006	0.2718 ± 0.0084	0.2789 ± 0.0086	0.3282 ± 0.0009	0.1180 ± 0.0040	0.1434 ± 0.0038	0.1788 ± 0.0005	0.0499 ± 0.0017	0.0543 ± 0.0015	0.0838 ± 0.0002
2.035 ± 0.007	-	-	-	0.0709 ± 0.0024	0.0840 ± 0.0022	0.1073 ± 0.0003	-	-	-
2.242 ± 0.007	-	-	-	0.0253 ± 0.0008	0.0307 ± 0.0008	0.0411 ± 0.0001	-	-	-
2.428 ± 0.007	0.1300 ± 0.0036	0.1267 ± 0.0090	0.1606 ± 0.0004	-	-	-	-	-	-
2.635 ± 0.007	0.0912 ± 0.0025	0.0937 ± 0.0028	0.1126 ± 0.0003	-	-	-	-	-	-
2.842 ± 0.007	0.0602 ± 0.0016	0.0593 ± 0.0018	0.0730 ± 0.0002	-	-	-	-	-	-
3.041 ± 0.008	0.0288 ± 0.0008	0.0286 ± 0.0009	0.0384 ± 0.0001	-	-	-	-	-	-
3.248 ± 0.008	0.0032 ± 0.0001	0.0032 ± 0.0001	0.0041 ± 0.0001	-	-	-	-	-	-

TABLE 11

Neutron Multiplication Measurements with 45.5% Enriched U-235 Slabs, Reflected on all Faces by Steel

Slab Thickness, in.	Inverse Neutron Multiplication								
	Effective Radius of Slab, in.								
	5.79			8.46			11.05		
	Counter 1	Counter 2	Counter 3	Counter 1	Counter 2	Counter 3	Counter 1	Counter 2	Counter 3
2.034 ± 0.007	-	-	-	-	-	-	0.1261 ± 0.0028	0.1487 ± 0.0030	0.1827 ± 0.0007
2.241 ± 0.007	-	-	-	-	-	-	0.0736 ± 0.0015	0.0828 ± 0.0018	0.1102 ± 0.0003
2.428 ± 0.007	-	-	-	0.1190 ± 0.0024	0.1319 ± 0.0026	0.1534 ± 0.0006	0.0316 ± 0.0007	0.0404 ± 0.0007	0.0479 ± 0.0002
2.635 ± 0.007	-	-	-	0.0696 ± 0.0014	0.0761 ± 0.0015	0.0952 ± 0.0003	-	-	-
2.842 ± 0.008	-	-	-	0.0297 ± 0.0006	0.0337 ± 0.0007	0.0388 ± 0.0001	-	-	-
3.041 ± 0.008	0.1548 ± 0.0029	0.1602 ± 0.0032	0.1868 ± 0.0007	-	-	-	-	-	-
3.642 ± 0.009	0.0627 ± 0.0011	0.0652 ± 0.0012	0.0717 ± 0.0003	-	-	-	-	-	-
3.849 ± 0.009	0.0339 ± 0.0006	0.0355 ± 0.0007	0.0411 ± 0.0002	-	-	-	-	-	-
4.056 ± 0.009	0.0087 ± 0.0001	0.0091 ± 0.0001	0.0104 ± 0.0001	-	-	-	-	-	-

TABLE 12

Neutron Multiplication Measurements with 45.5% Enriched U-235 Slabs, Reflected on all Faces by Aluminium

Slab Thickness, in.	Inverse Neutron Multiplication								
	Effective Radius of Slab, in.								
	5.79			8.46			11.05		
	Counter 1	Counter 2	Counter 3	Counter 1	Counter 2	Counter 3	Counter 1	Counter 2	Counter 3
1.827 ± 0.006	-	-	-	0.3543 ± 0.0062	0.3493 ± 0.0058	0.3742 ± 0.0014	0.2494 ± 0.0063	0.2503 ± 0.0080	0.2946 ± 0.0016
2.428 ± 0.007	-	-	-	0.1675 ± 0.0028	0.1726 ± 0.0028	0.1885 ± 0.0007	0.0718 ± 0.0012	0.0725 ± 0.0012	0.0890 ± 0.0003
2.635 ± 0.007	-	-	-	0.1142 ± 0.0019	0.1134 ± 0.0018	0.1338 ± 0.0005	0.0209 ± 0.0003	0.0229 ± 0.0004	0.0292 ± 0.0001
3.041 ± 0.008	-	-	-	0.0298 ± 0.0007	0.0301 ± 0.0007	0.0358 ± 0.0002	-	-	-
3.642 ± 0.009	0.0993 ± 0.0015	0.1008 ± 0.0015	0.1052 ± 0.0004	-	-	-	-	-	-
3.849 ± 0.009	0.0686 ± 0.0010	0.0683 ± 0.0010	0.0748 ± 0.0003	-	-	-	-	-	-
4.056 ± 0.009	0.0417 ± 0.0006	0.0409 ± 0.0006	0.0452 ± 0.0002	-	-	-	-	-	-
4.255 ± 0.010	0.0176 ± 0.0002	0.0186 ± 0.0003	0.0200 ± 0.0001	-	-	-	-	-	-

TABLE 13

Estimated Critical Thicknesses of Slabs

Reflector System	Effective Radius of Slab, in.		
	5.79	8.46	11.05
"Bare"	7.26 ± 0.03	5.47 ± 0.04	Not measured
Natural Uranium	3.27 ± 0.02	2.36 ± 0.02	2.01 ± 0.02
Graphite	3.00 ± 0.02	2.14 ± 0.02	1.78 ± 0.02
Borated Graphite	3.76 ± 0.03	2.80 ± 0.03	2.40 ± 0.02
Steel	4.12 ± 0.03	2.98 ± 0.02	2.57 ± 0.02
Aluminium	4.40 ± 0.02	3.21 ± 0.02	2.72 ± 0.02

TABLE 14

Reflector System	Critical Height, in. Effective Radius of Slabs, in. 5.79			8.46			11.05			(a) Best Fit for B^2, λ_1 and λ_2			(b) Best Fit for λ_1 and λ_2, Using $B^2 = 0.204$, in.$^{-2}$	
	Experimental	Calculated Using Constants (a)	Calculated Using Constants (b)	Experimental	Calculated Using Constants (a)	Calculated Using Constants (b)	Experimental	Calculated Using Constants (a)	Calculated Using Constants (b)	B^2, in.$^{-2}$	λ_1, in.	λ_2, in.	λ_1, in.	λ_2, in.
"Bare"	7.26 ± 0.03	7.32	7.44	5.47 ± 0.04	5.41	5.39	Not Measured	4.89	4.83	0.219	1.25	1.25	1.43	1.43
Natural Uranium	3.27 ± 0.02	3.27	3.27	2.36 ± 0.02	2.36	2.36	2.01 ± 0.02	2.02	2.02	0.200	3.06	2.79	2.96	2.75
Graphite	3.00 ± 0.02	3.01	3.05	2.14 ± 0.02	2.12	2.12	1.78 ± 0.02	1.79	1.77	0.214	2.77	2.77	2.88	2.88
Borated Graphite	3.76 ± 0.03	3.76	3.76	2.80 ± 0.03	2.79	2.78	2.40 ± 0.02	2.42	2.42	0.193	3.06	2.67	2.77	2.56
Steel	4.12 ± 0.03	4.14	4.10	2.98 ± 0.02	2.97	2.98	2.57 ± 0.02	2.56	2.59	0.196	2.59	2.59	2.48	2.48
Aluminium	4.40 ± 0.02	4.42	4.35	3.21 ± 0.02	3.17	3.18	2.72 ± 0.02	2.74	2.77	0.192	2.55	2.55	2.40	2.40

TABLE 15

Estimated Dimensions of the Critical Slab and Sphere

($B^2 = 0.204$ in.$^{-2}$)

System	λ, in.	Infinite Slab Critical Thickness, in.	Sphere		Reflector Thickness, in.
			Critical Radius in.	Critical Mass, kg	
Unreflected	1.43	4.10	5.52	209	0
U Nat Reflector	2.96	1.03	3.99	79	7
Graphite Reflector	2.88	1.20	4.07	84	6
Borated Graphite Reflector	2.56	1.84	4.40	106	8
Steel Reflector	2.48	1.98	4.47	111	6
Aluminium Reflector	2.40	2.16	4.55	118	6

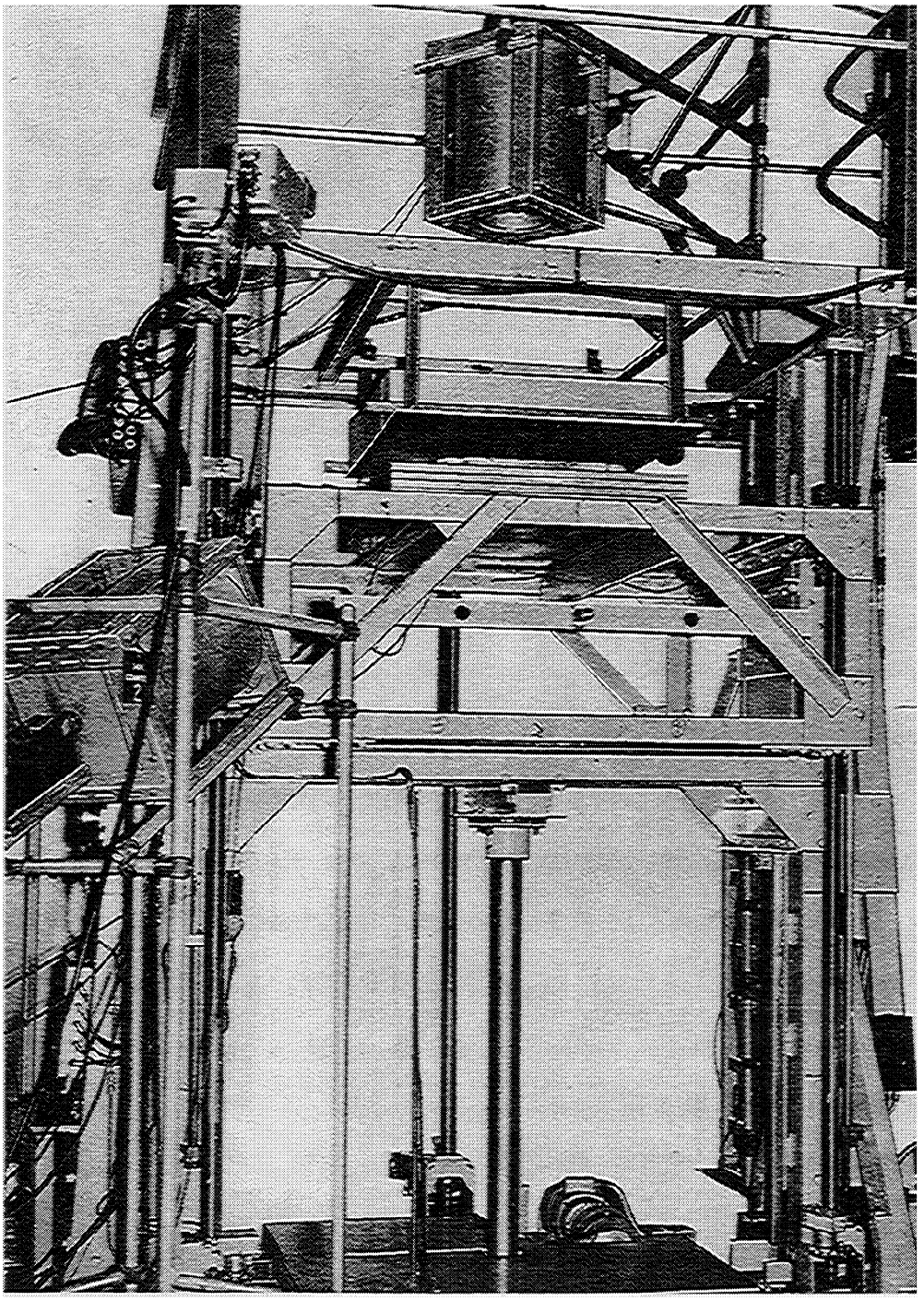

FIGURE 1. ATLAS

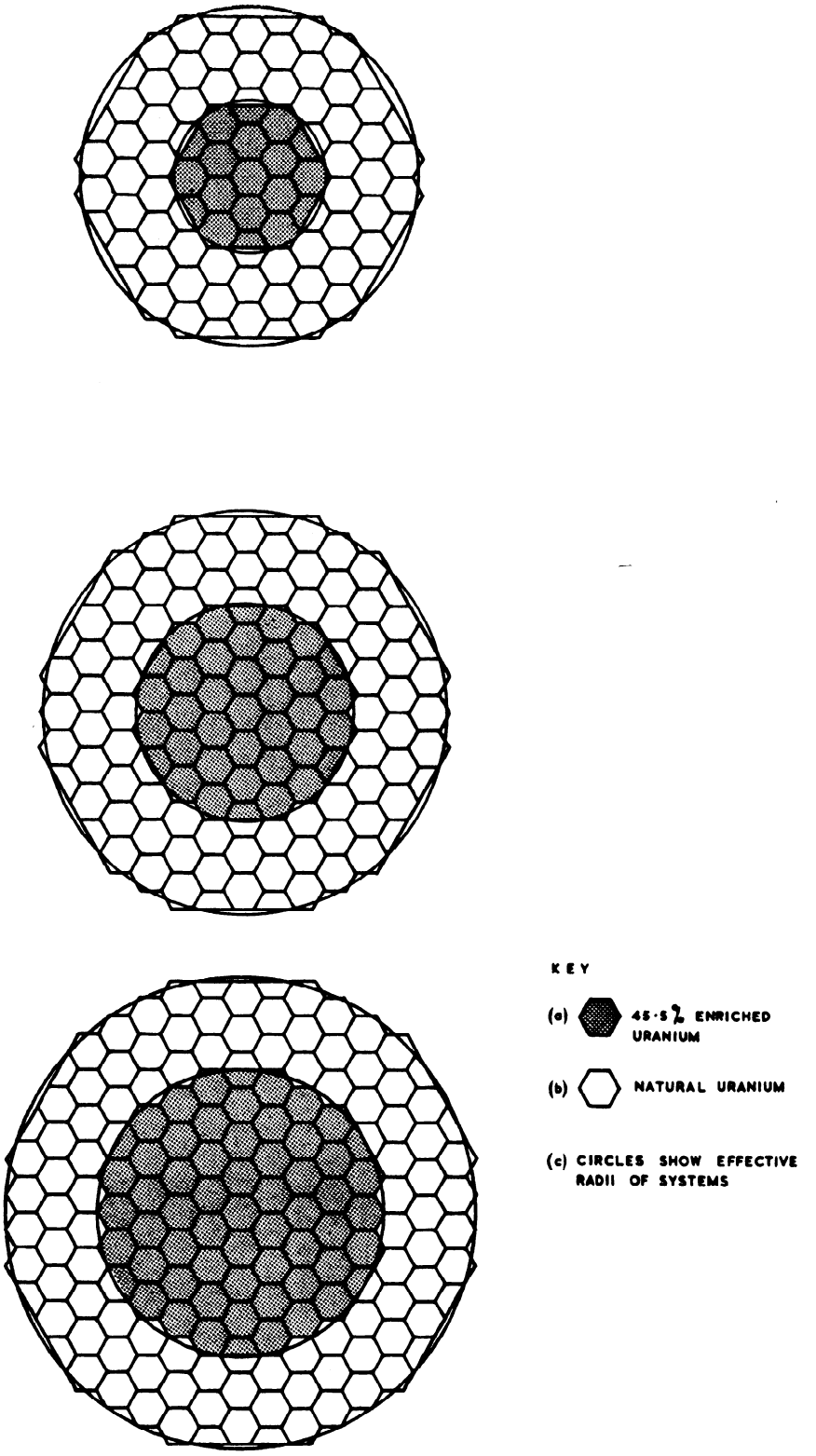

FIGURE 2. ENRICHED URANIUM PSEUDO CYLINDERS AND NATURAL URANIUM SIDE REFLECTOR DIAGRAMMATIC

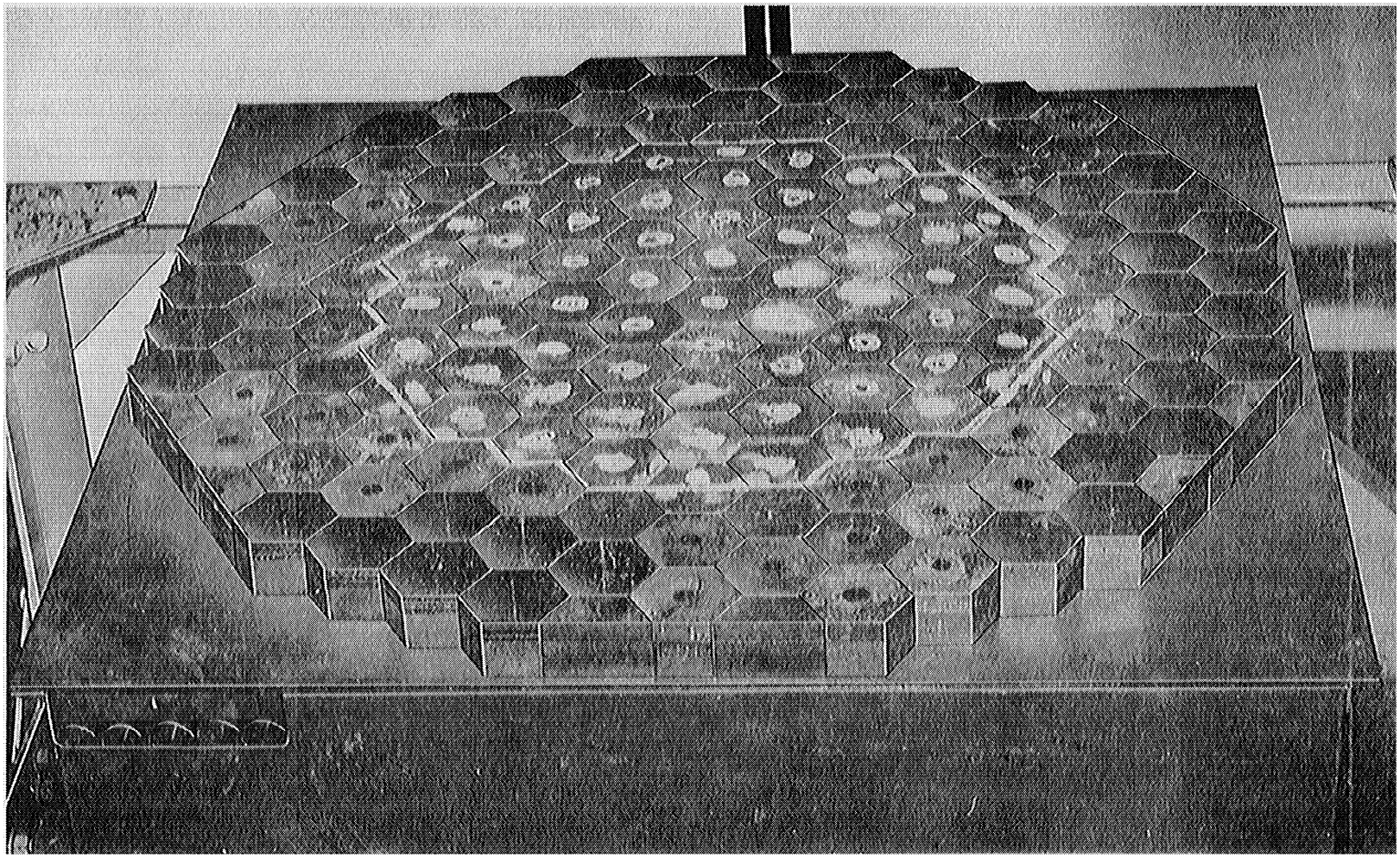

FIGURE 3. ENRICHED URANIUM CORE NATURAL URANIUM BOTTOM AND SIDE REFLECTORS

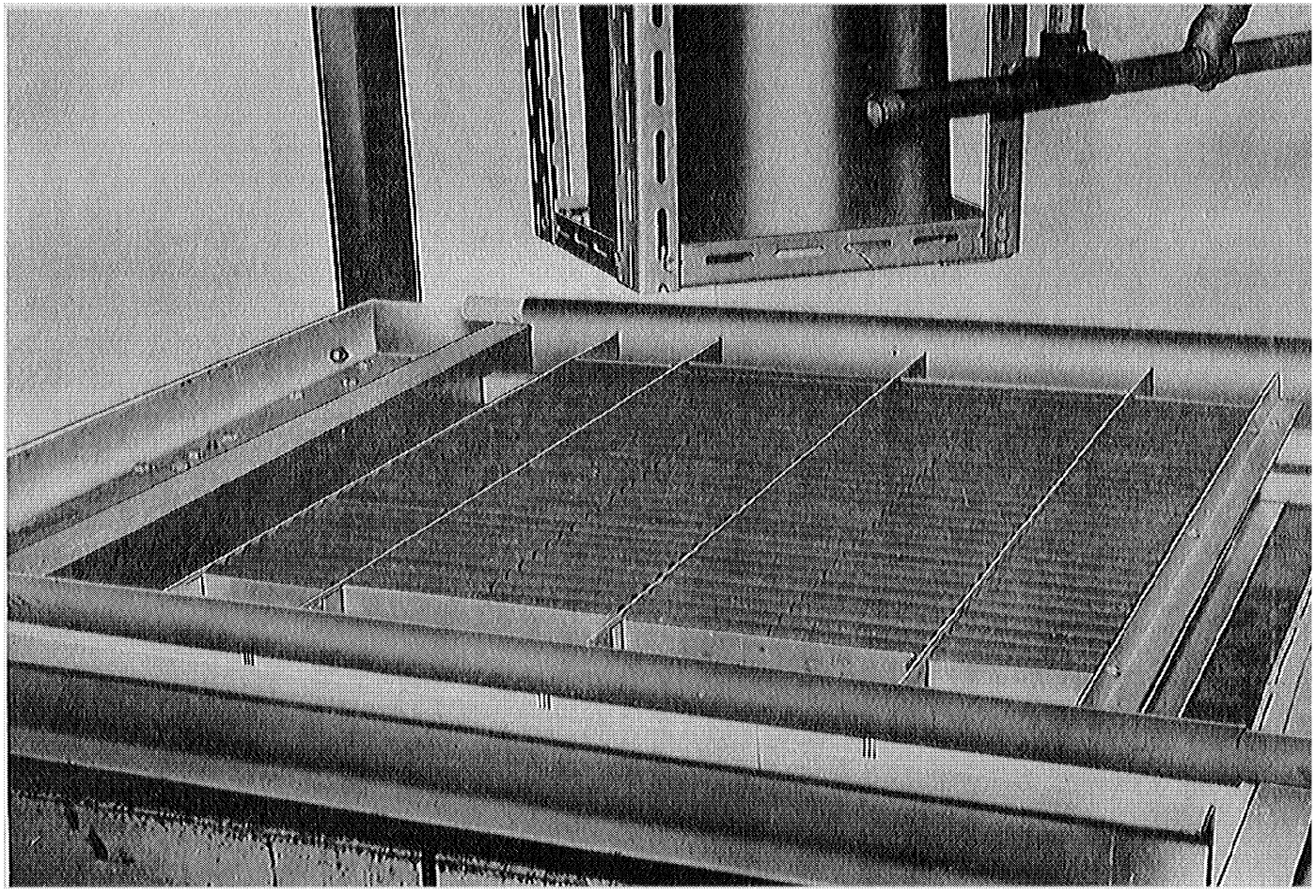

FIGURE 4. UPPER NATURAL URANIUM REFLECTOR

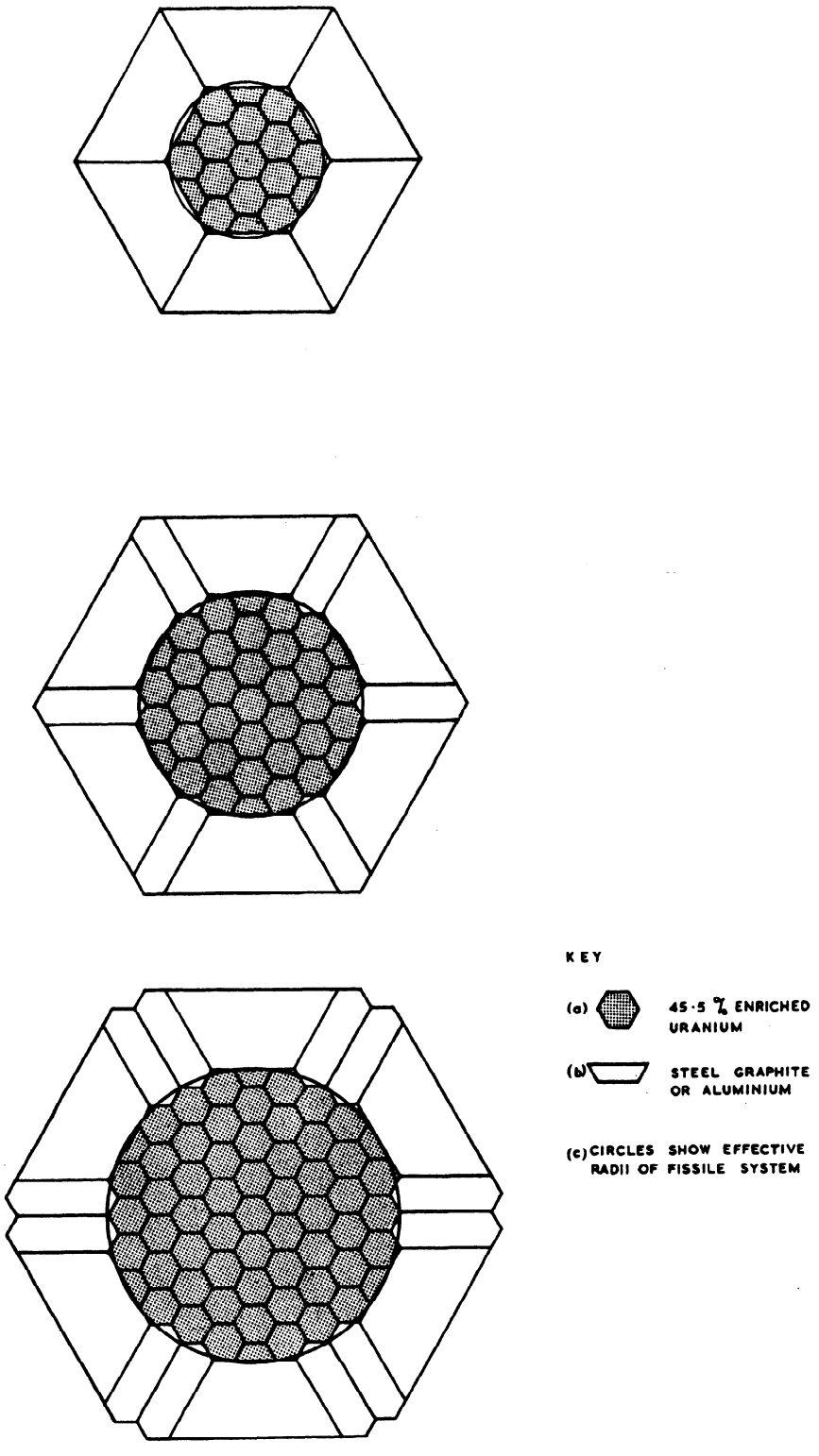

FIGURE 5. SIDE REFLECTOR OF GRAPHITE STEEL AND ALUMINIUM. DIAGRAMMATIC

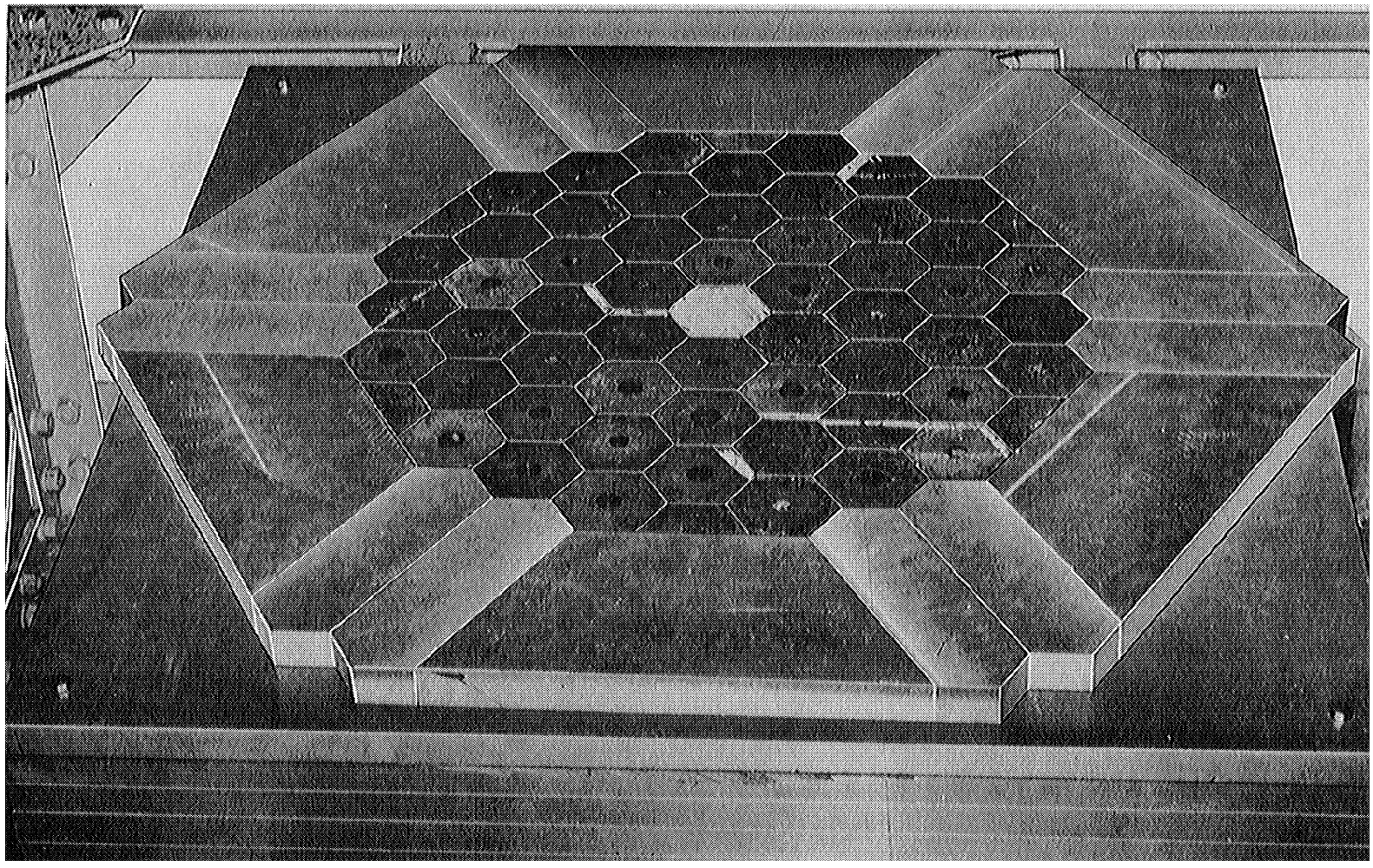

FIGURE 6. ALUMINIUM REFLECTED ASSEMBLY

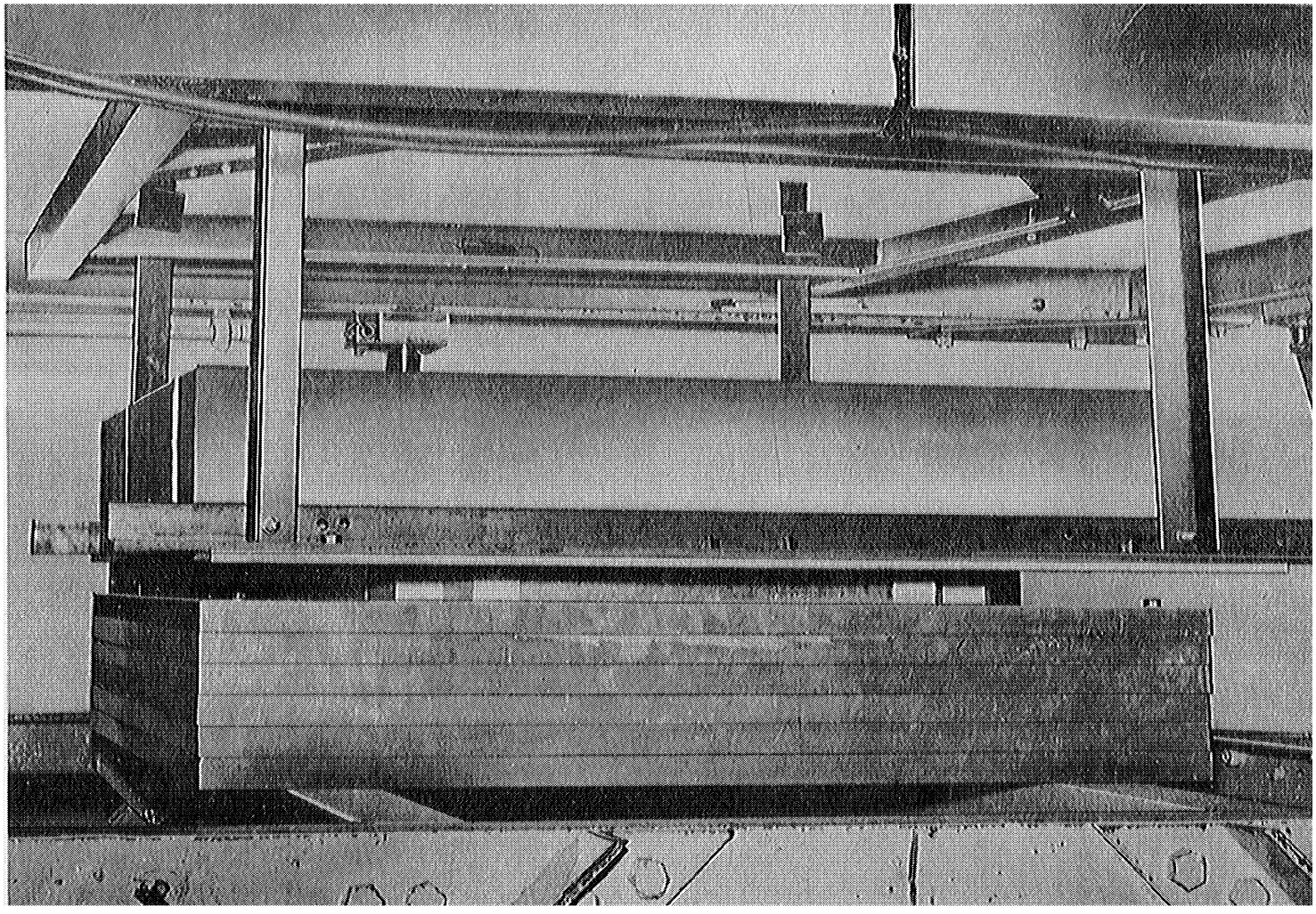

FIGURE 8. ALUMINIUM REFLECTED ASSEMBLY

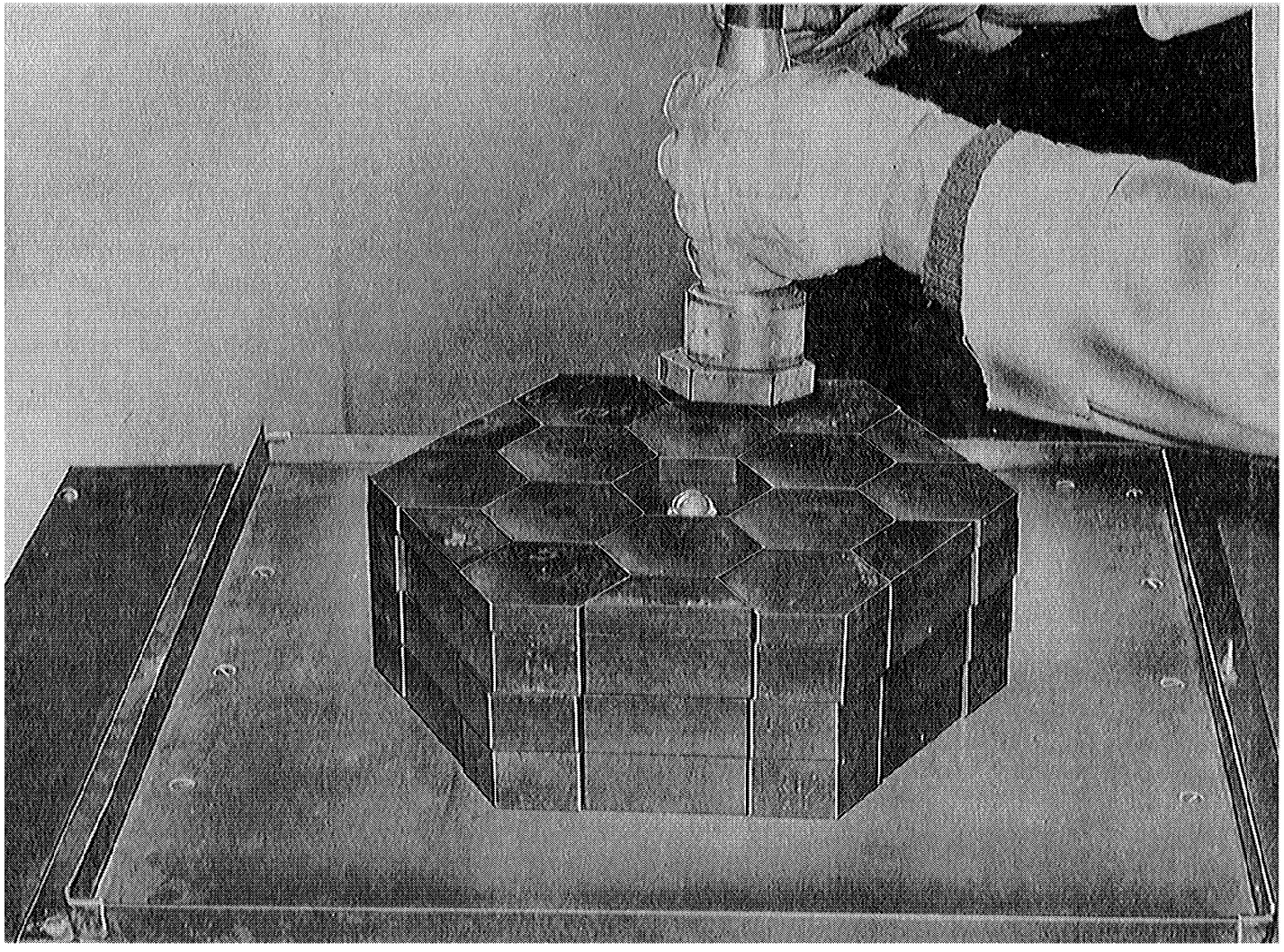

FIGURE 9. "BARE" ASSEMBLY SHOWING MOCK FISSION NEUTRON SOURCE

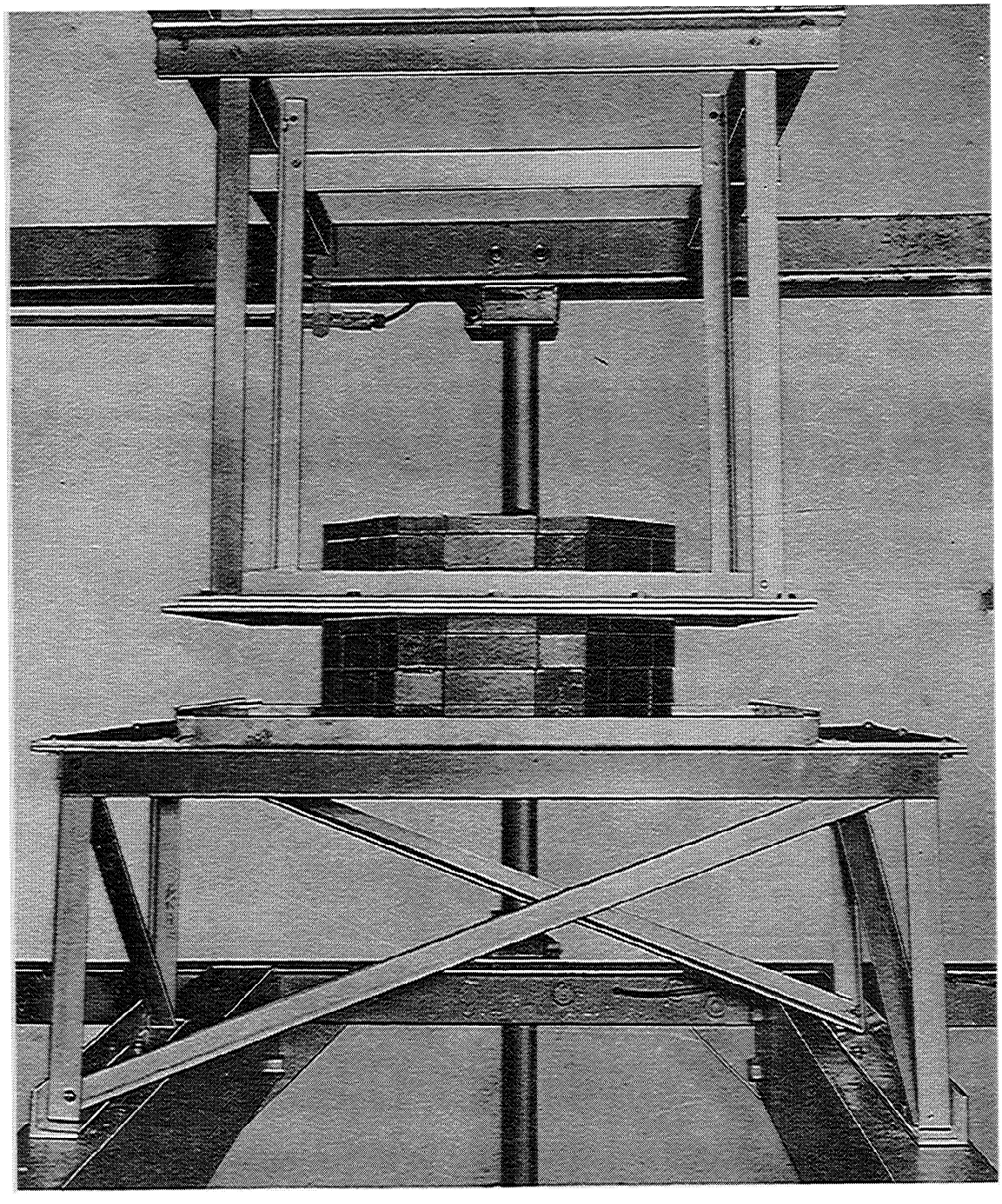

FIGURE 10. COMPLETE "BARE" ASSEMBLY - SHOWING ADDITIONAL INTERLEAVED PLATES

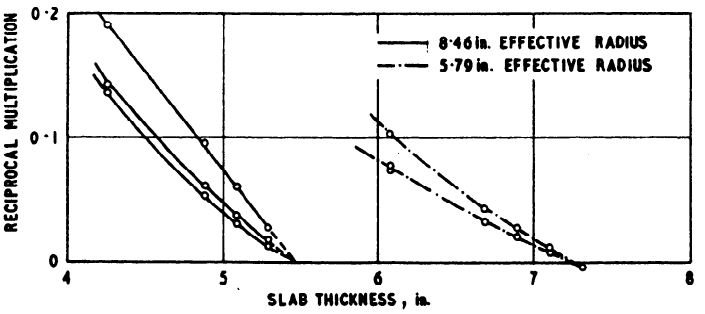

(a) 45·5 % U-235 SLABS BARE

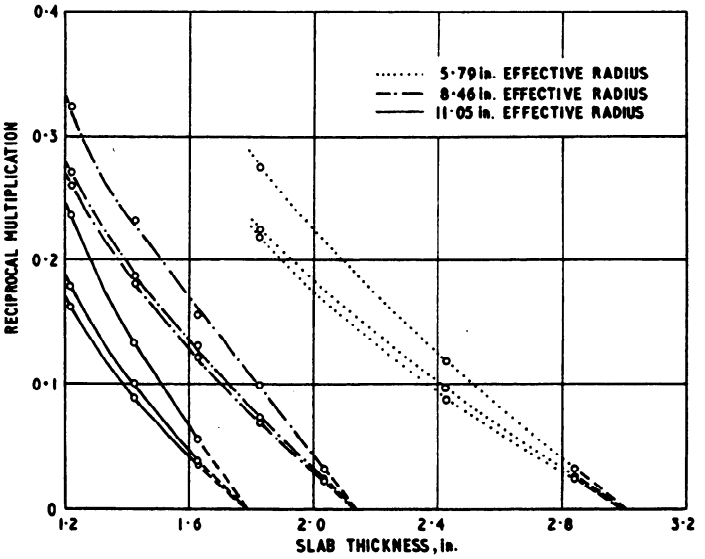

(b) 45·5 % U-235 SLABS, REFLECTED ON ALL FACES BY GRAPHITE

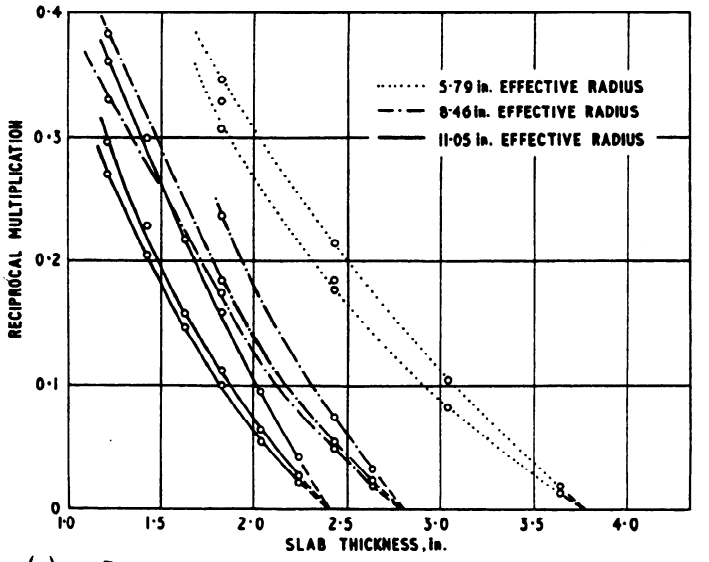

(c) 45·5 % U-235 SLABS, REFLECTED ON SLAB FACES BY BORATED GRAPHITE AND ON SIDE FACES BY GRAPHITE

FIGURE II. RECIPROCAL MULTIPLICATION CURVES FOR "BARE" GRAPHITE AND BORATED GRAPHITE REFLECTED ASSEMBLIES

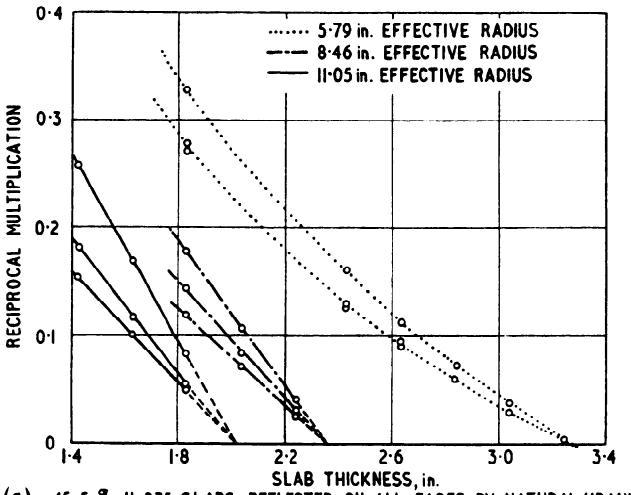

(a) 45·5 % U-235 SLABS, REFLECTED ON ALL FACES BY NATURAL URANIUM

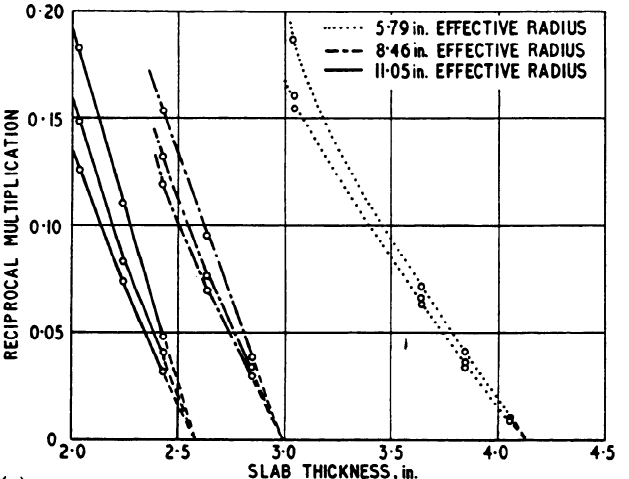

(b) 45·5 % U-235 SLABS, REFLECTED ON ALL FACES BY STEEL

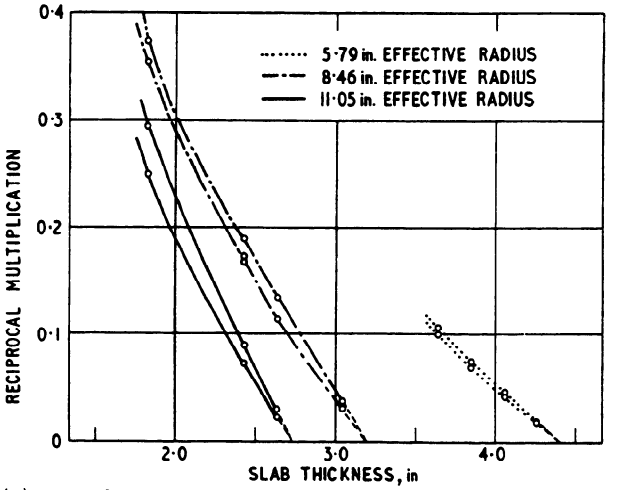

(c) 45·5 % U-235 SLABS, REFLECTED ON ALL FACES BY ALUMINIUM

FIGURE 12. RECIPROCAL MULTIPLICATION CURVES FOR NATURAL URANIUM, STEEL AND ALUMINIUM REFLECTED ASSEMBLIES